Electronic structure of silver and copper ultrathin films on V(100): Quantum-well states

T. Valla, P. Pervan, and M. Milun
Institute of Physics, P.O. Box 304, 10000 Zagreb, Croatia

A. B. Hayden and D. P. Woodruff
Physics Department, University of Warwick, Coventry CV4 7AL, United Kingdom

(Received 10 January 1996; revised manuscript received 26 June 1996)

Angular-resolved photoemission and inverse-photoemission spectroscopies have been used to investigate the valence-electron states in ultrathin films of silver and copper deposited on a V(100) surface. For both noble metals, discrete *s*-*p* derived states are observed within the Δ_1 gap of the vanadium substrate (approximately ± 2 eV around E_F). These states are analyzed using a simple quantum-well picture. For a pseudomorphically grown (centered tetragonal) silver film in the bulklike limit we have determined k_F (1.19 Å^{-1}) and the energies of critical points, X_1 (7.60 $\pm$ 0.15 eV) and $X_{4'}$ (2.5 $\pm$ 0.3 eV) in the $E(k)$ dispersion of the Δ_1 band in the Γ-Δ-X direction. The bottom of the Δ_1 band, i.e., Γ_1 point, was estimated to be -6.4 ± 0.3 eV by fitting the experimentally determined points with a free-electron parabola. In the case of copper overlayers, it was not possible to determine the dispersion of the bulklike Δ_1 band because Cu films thicker than two monolayers showed poor order. At low coverages (1–2 ML) of both silver and copper, we find that dispersion in $k_\parallel$ of the discrete *s*-*p* quantum-well states is described by a significantly enhanced electron effective mass ($m^* > 2m_e$). This is interpreted as due to strong hybridization of these states with the *d* derived states of the vanadium substrate. [S0163-1829(96)08139-8]

I. INTRODUCTION

In the past decade, there has been considerable interest in the magnetic properties of surfaces, thin films, and superlattices,[1,2] which include a transition-metal constituent. These systems can display some very interesting phenomena. For example, magnetic superlattices such as Co/Cu/Co(100) and Fe/Ag/Fe(100) (Ref. 3) show an oscillatory and long-range (20–30 atomic layers) magnetic coupling of the magnetic layers through the intervening nonmagnetic layers. Such a long-range coupling cannot be explained in terms of the spin-dependent *d*-*d* hybridization at the interface. The interface moment that would result from such a mechanism is calculated[4] to be very small ($<0.1\mu_B$) for noble metals on 3*d* ferromagnetic metals, and is expected to decay very rapidly away from the interface. On the other hand, spin-dependent coupling can induce spin polarization of the more delocalized *s*-*p* states. These states extend over much longer distances, and therefore can mediate the long-range indirect coupling between the magnetic layers.

Within a simple quantum-well (QW) state picture for the *s*-*p* derived states, it is possible to provide a magnetic coupling mechanism in magnetic superlattices.[3,5] QW states are created by trapping the electrons in a thin film. The surface barrier, on the vacuum side, and a band gap for propagating *s*-*p* states, on the substrate side, confine the *s*-*p* electrons within the film. When the film thickness is comparable to the electron wavelength, these states appear at discrete energies with quantized wave vectors perpendicular to the film. Within the phase-accumulation model,[6] the quantization condition for the existence of such a state follows from

$$\Phi_B + 2\Phi_D + \Phi_C = 2\pi m, \tag{1}$$

where m is the quantum number of the state, Φ_B and Φ_C are the phase shifts upon reflection at the surface barrier and at the interface, respectively, while $\Phi_D = Nkd$ is the phase change accumulated in traversing the film. N is the number of atomic layers in the film, d is the distance between the layers, and k is the wave vector perpendicular to the film. Within a simple model[6–8] it is possible to evaluate the explicit energy dependence of all phase shifts appearing in Eq. (1), and accordingly predict the energies of the QW states. For example, the image barrier approximation for the surface barrier gives[6–8]

$$\Phi_B/\pi = [(3.4)/(E_V - E)]^{1/2} - 1. \tag{2}$$

On approaching the vacuum level (E_V), Φ_B diverges, leading to an infinite set of (Rydberg-like) solutions of Eq. (1); these higher m states are the so-called image states. On the other hand, the interface phase shift (Φ_C) must increase by π on traversing from the bottom to the top of the gap, independent of the detailed nature of the gap;[9] Φ_C changes more rapidly near the edges of the gap than at its center.

In the case of a ferromagnetic substrate, the interface phase change Φ_C may be spin-dependent because of the relative displacement of the minority and majority substrate subbands and their corresponding gaps, and thus differences in energy relative to the gap edges for the two spin polarizations. This can result in different interface phase changes at the same energy, and consequently [see Eq. (1)], in a spin polarization of the QW states. For some superlattices[3,10] the oscillation period of the magnetic coupling is found to be equal to the periodicity of the appearance of spin-polarized QW states at the Fermi level, indicating that the QW states may be responsible for the transmission of the magnetic coupling through the nonmagnetic layers.

The simple QW description given above assumes, of course, that the thin film can be treated as a homogeneous medium, and that the QW states are simply the stationary states corresponding to standing waves perpendicular to the surfaces. At film thicknesses of only a single monolayer, in particular, one might anticipate the need for a more sophisticated approach.[11] Recent first-principles calculations show that substrate, adsorbate, and interface states can be resolved in the monolayer case,[12,13] depending on the location of the charge. The interface states that originate from the overlayer can be regarded as precursors of the quantum-well states for thicker overlayers.

In this work we present angular-resolved photoemission and momentum-resolved inverse photoemission data recorded from ultrathin films of silver and copper deposited onto a vanadium (100) surface. The growth modes of these films are well documented.[14–16] A relatively small lattice mismatch (4%) between the fcc Ag(100) and bcc V(100) planes, and a small surface free energy for Ag (1.3 Jm^{-2}), result in pseudomorphic ''layer-by-layer'' growth of the first 5–10 atomic layers at a substrate temperature around 300 K.[14,15] The implied local structure of the silver film is shown schematically in Fig. 1(c). In the case of copper, the conditions for such a growth are rather unfavorable, with a lattice mismatch of approximately 16% and a significantly larger Cu surface free energy (1.9 Jm^{-2}). Consequently, only the first two atomic layers are found to grow in registry with the substrate, and even then the degree of disorder of the film is much higher than in the Ag films.[16] For higher Cu coverages, disordered growth, structural changes, and clustering, make QW analysis impossible.

Good layer-by-layer growth is a necessary, but not a sufficient, condition for the existence of the discrete overlayer QW states. A further requirement is that there should be a band gap in the substrate to ensure reflection of propagating *s-p* overlayer states, and thus their confinement within the film. Vanadium fulfills this substrate requirement. As can be seen in Fig. 1(a),[17] there is a Δ_1 *s-p* hybridization gap (in the following we refer to this as the Δ_1 gap) in the V band structure in the range of approximately ± 2 eV around E_F. Figure 1(b) (Ref. 18) shows the band dispersion in bulk fcc silver along the Γ-Δ-X direction. It is easy to see that the lower branch of the Δ_1 band in Ag coincides with the Δ_1 gap of the V substrate, providing the necessary conditions in this energy range for Ag QW *s-p* states in thin Ag films grown on V(100).

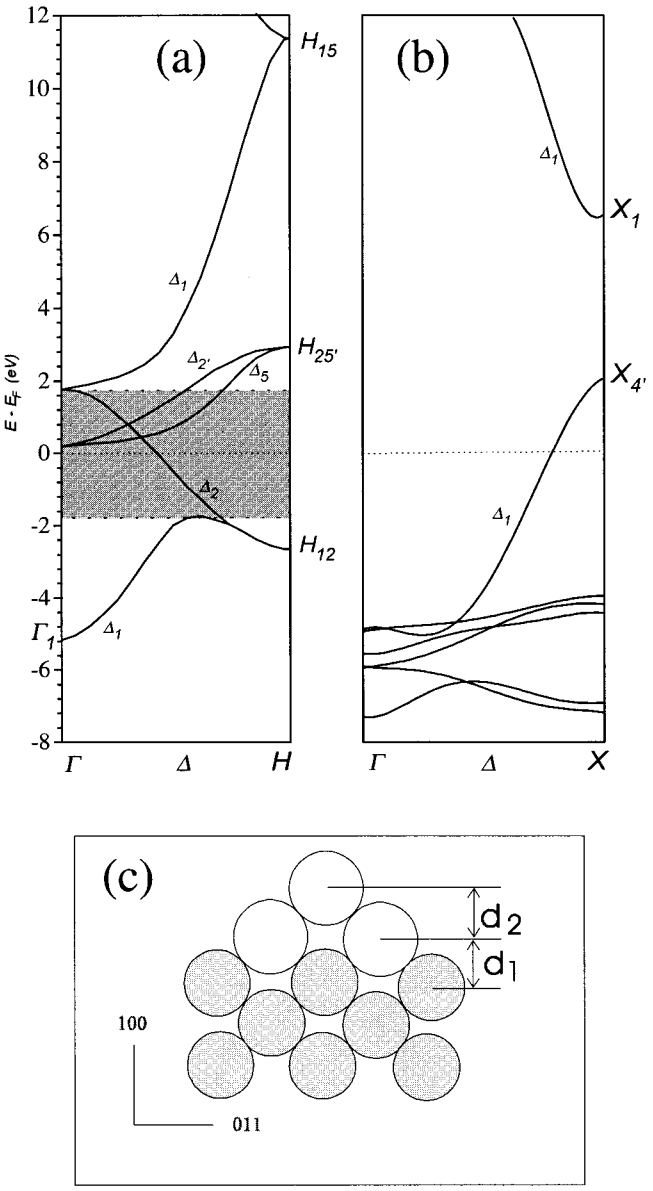

FIG. 1. The calculated energy bands of vanadium (Ref. 17) (a) and fcc silver (Ref. 18) (b) along the Γ-Δ-*H* and Γ-Δ-*X* directions, respectively, of the bulk Brillouin zones, which correspond to the normal to (100) surfaces. Note the existence of the Δ_1 gap in the band structure of vanadium (shadowed area) (c) ⟨110⟩ sectional view of the structure of the tetragonal centred phase of silver or copper expected for pseudomorphic growth on a V(100) surface. If relaxation effects are excluded, the interlayer separations d_1 and d_2 are 1.74 and 1.94 Å for silver and 1.45 and 1.38 Å for copper, respectively.

II. EXPERIMENTAL DETAILS

The experiments were carried out in two separate experimental chambers. The first one, in which angle-resolved ultraviolet photoelectron spectroscopy (ARUPS) was performed, was equipped with a 180° concentric hemispherical analyzer (VSW HA 100) and a He discharge lamp. The energy resolution of the analyzer was 180 meV and the angular resolution was $\pm 2.5°$. A He I (21.2 eV) resonance gas discharge lamp provided the photon excitation. The positions of both the electron-energy analyzer and the discharge lamp were fixed relative to the chamber, and different emission angles were obtained by rotation of the sample.[19] The momentum-(*k*-) resolved inverse photoemission spectroscopy (KRIPES) experiments were carried out in a second purpose built UHV system fitted with a LiF lens as a dispersing element and two separate photon detectors installed on the optical axis to record simultaneous isochromat spectra at 10.0- and 11.5-eV photon energies.[20] The spectral resolution at these two photon energies was 0.6 and 0.4 eV, respectively, and angular spread of the low-energy electron source that defines the momentum resolution parallel to the surface was approximately $\pm 5°$.[20]

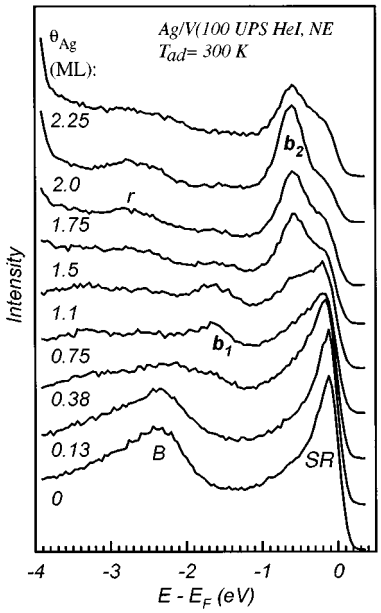

FIG. 2. Photoemission spectra from thin (up to 2.5-ML coverage) silver films on V(100). The spectra are recorded at normal emission ($k_{\|} = 0$). SR denotes the peak due to the surface resonance of the clean V(100) surface, B labels the feature due to emission from the vanadium bulk s-p band (Δ_1 symmetry), while b_1, b_2, and r are the features due to discrete overlayer states.

Both experimental systems were additionally equipped with low-energy electron diffraction optics and the ability to record Auger electron spectra using concentric hemispherical analyzers. The vanadium sample was mounted on the sample holder with the plane of electron emission or incidence corresponding to the ΓNPH plane of the bulk Brillouin zone of vanadium; the normal emission and normal incidence experiments ($k_{\|} = 0$) thus probed the states along the Γ-Δ-H and Γ-Δ-X high-symmetry lines of the substrate and overlayer, respectively. Extensive argon sputtering and annealing cycles were used to ensure an atomically clean and well ordered vanadium surface (the details are described elsewhere[21]). The silver and copper films were evaporated from tungsten baskets at rates of approximately 1/5 ML per minute. Overlayer thicknesses were determined using Auger electron spectroscopy (AES) and thermal desorption spectroscopy (TDS); the values obtained were found to be in agreement with those determined by observation of the discrete overlayer states in ARUPS and KRIPES.

III. RESULTS AND DISCUSSION

A. Ag/V(100)

We have examined the valence-band energy region of the Ag/V(100) system by both ARUPS and KRIPES in the wide range of Ag film thicknesses up to 15 ML. Normal emission photoemission spectra from films of different thicknesses in the low coverage part of this range are shown in Fig. 2. The photoemission spectrum of the clean V(100) surface (shown at the bottom of the figure), is characterized by a direct transition from the bulk s-p band (Δ_1 symmetry[19]) at approximately -2.4 eV relative to E_F (marked as B), and a pronounced surface resonance emission, close to the Fermi level

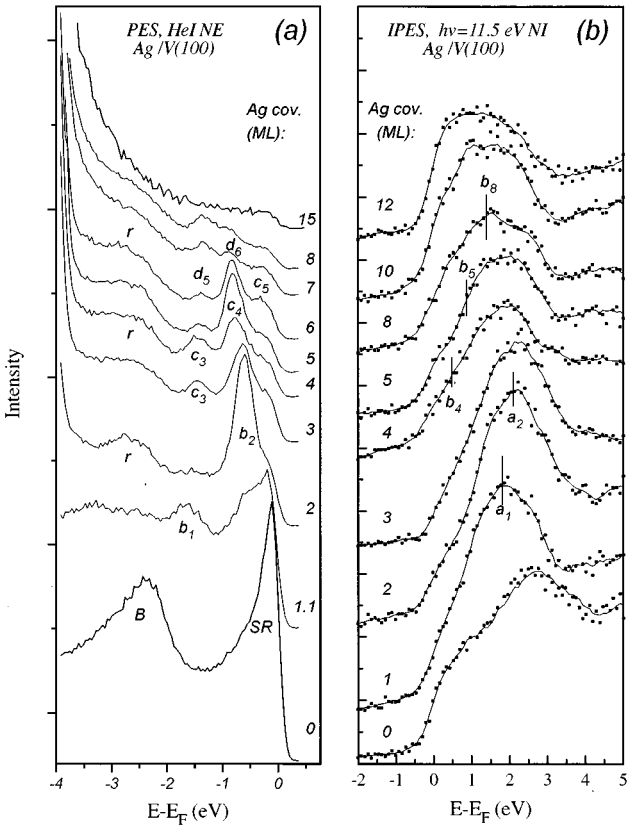

FIG. 3. Normal emission photoelectron spectra (a), and normal incidence inverse photoelectron spectra (b) from Ag films grown on V(100) to various coverages (labeled in ML units). Energies are relative to the Fermi level.

(marked as SR).[22] As expected, this resonance is strongly attenuated by Ag deposition. At the same time, a new feature (b_1) appears at approximately -1.6 eV. Around 1 ML coverage, the vanadium surface resonance completely disappears, while the intensity of the b_1 peak reaches its maximum. With further silver deposition, the intensity of this state is gradually attenuated and simultaneously a new peak (b_2) appears at approximately -0.6 eV; this peak has its maximum intensity at a thickness corresponding to the completion of the second silver monolayer. These two peaks are attributed to s-p character Ag-derived quantum-well states, as discussed below. The further appearance of new QW states as a function of increasing film thickness can be followed up to coverages of approximately 10 ML of Ag, by ARUPS, as shown in Fig. 3(a). In the photoemission spectra [Fig. 3(a)], several QW states can be clearly resolved: b_1, b_2, c_3, c_4, c_5, d_5, and d_6 (the notation is explained later in the text). Note that the c and d states exist at more than one nominally integral value of the number of layers in the film. Since the quantization condition (1) defines the energy of a given state in terms of the corresponding film thickness Nd, we deduce that after the first 2–3 layers the growth mechanism is not strictly layer-by-layer, and that the ''growth front'' (the number of uncompleted layers during the growth) is around three atomic layers. In the inverse photoemission spectra [Fig. 3(b)], there are no such clearly resolved overlayer states. This can be largely attributed to the fact that both the signal-to-noise ratio and the energy resolution of the

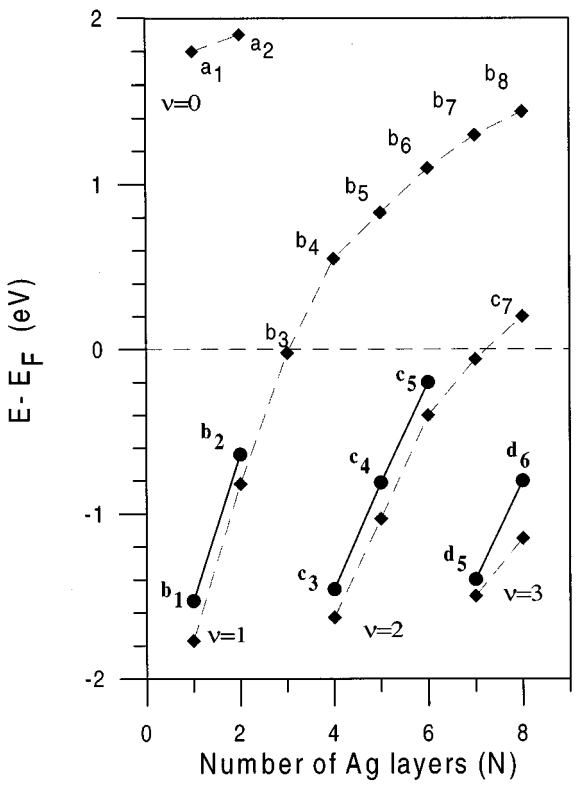

FIG. 4. Energies (relative to E_F) of the observed and calculated overlayer states for Ag on V(100) at various coverages (Fig. 3, see text). The assignments of the states are defined by $\nu = N - m$, where N denotes number of Ag layers and m is the quantum number of wave-function nodes of the state inside the quantum well. Theoretically calculated points and experimentally observed QW states are represented by diamonds and circles, respectively.

KRIPES data are inferior to those of the ARUPS measurements. Therefore, instead of attributing the features in the spectra to specific QW states we only indicate points in the spectra where QW states are predicted to occur above the Fermi level by theoretical calculations[25] which yield occupied QW states close to those seen in our ARUPS data. Although there is correspondence between some of the calculated values and the position of intensity maxima in the KRIPES spectra, we use only QW states observed in photoemission in order to estimate the $E(k)$ dispersion curve (Fig. 7) later in the text.

The QW states observed in the spectra shown in Fig. 3(a) may be characterized by their quantum number m, as suggested by Eq. (1). However, another quantum number, $\nu = (N - m)$, is usually[23,24] used. Fig. 4 summarizes the characteristics of the observed QW states deduced from the data of Fig. 3. The states associated with the same ν value are connected with solid lines. Their energies are in very good agreement with the theoretically calculated values[25] (Fig. 4, squares connected with dashed lines).

The notation used in Fig. 3 is based on a combination of the m and ν quantum numbers. States with $\nu = 0, 1, 2, 3, \ldots$, are labeled $a, b, c, d, \ldots$, respectively, while a subscript is added to indicate increasing m values; the lowest energy states ($m = 0$) are given a subscript of 1, which leads to general subscript values of $(m+1)$. Accordingly, we resolve $b_1 - b_2$, $c_3 - c_5$, and $d_5 - d_6$ states within the Δ_1 band-gap energy range. If we look back at Fig. 3(a), we see that the peaks closest to the Fermi level (e.g., b_2 and c_4) are more pronounced and sharper than the peaks at lower energies (e.g., states b_1, c_3, and d_5). We believe the overlayer state marked b_2 ($\nu = 1$ at 2 ML) to be the clearest and most intense QW state of any published in the literature so far. Upon correcting for the experimental resolution (≈ 180 meV), the estimated intrinsic lifetime broadening is ≈ 250 meV. This value is nearly the same as that of Shockley surface states at approximately the same binding energies on noble metal surfaces.[26] Generally, the width of the QW states can be understood in terms of the energetic position of the state within the Δ_1 gap of vanadium [see Fig. 1(a)]. The extension of the wave functions of the state into the classically forbidden region outside the well is determined by the imaginary part of the wave vector that is proportional to the square root of the well depth (or, in our case, to the energetic displacement from the gap edge).[6–8] The states closest to the gap edge penetrate furthest into the solid and thus are best able to hybridize with the substrate propagating states, leading to shorter lifetimes and broader peaks. In the present case, the Fermi level lies at the center of the gap, so surface-localized states close to the Fermi level should have the longest lifetimes and give the narrowest peaks.

The broad features in Fig. 3(a), marked r, are probably due to overlayer resonances, which, because they fall outside the band gap, can hybridize with the vanadium Δ_1 band (see Fig. 1). Figure 5(a) shows the low-energy component of the photoemission spectra recorded from the thin Ag films on V(100); the highest-energy components of these spectra are those shown in Fig. 3(a). In the lowest-energy range we expect the spectra to be dominated by true secondary electrons resulting from the inelastic cascade initiated by the photoemission process; in the bulklike limit this secondary electron spectrum should reflect the one-dimensional density of final states (above the vacuum level) along the symmetry line of detection.[27] The broad features seen between 9 and 12 eV above the Fermi level [marked r' in Fig. 5(a)] correspond to transitions into overlayer-derived final states along the Γ-Δ-H and Γ-Δ-X symmetry lines of the substrate and overlayer. As we can see from Fig. 1(b), this energy region corresponds to s-p derived states that form the upper branch of the Δ_1 bulk Ag band.

The top spectrum in Fig. 5(a) is recorded from a 15-ML-thick silver film (still showing the substrate lateral periodicity). Further silver deposition does not change the shape of the secondary emission, implying that the bulklike limit has been reached. This secondary emission can thus be related to the one-dimensional density of final states of pseudomorphic Ag in the Γ-Δ-X direction. The steplike increase of the secondary emission at approximately 3.5 eV above the onset at the vacuum level can be assigned to the bottom of the upper Δ_1 band at the X_1 point. A strictly one-dimensional density of states (DOS) has a singularity at the zone boundary, so we might expect a peak rather than a step in the secondary emission intensity at the X_1 point. However, this potential peak is probably washed out by the finite angular and energy resolution of the experiment. In many cases[28,29] the intensity increase (or decrease) inflection point has been found to provide a more reliable determination of the energy of the

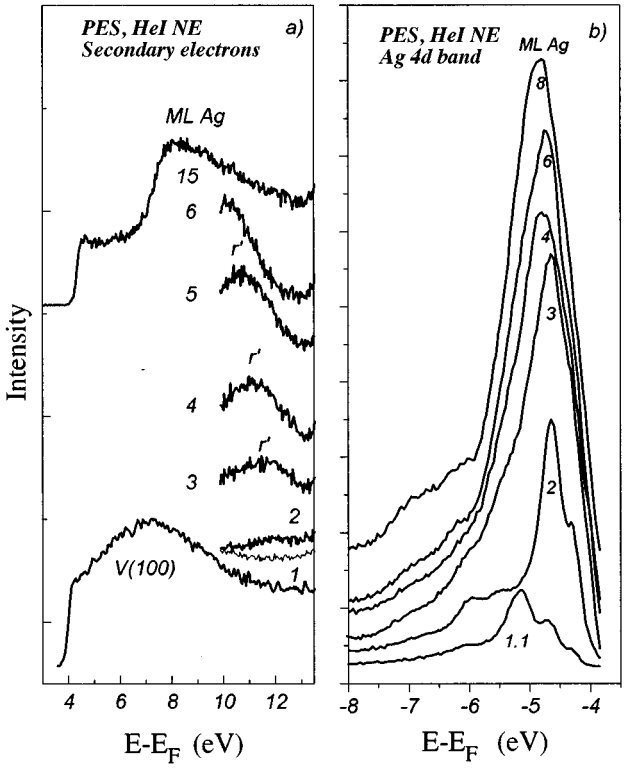

FIG. 5. (a) The secondary electron region and (b) the Ag 4*d* valence-band regions of some of the same photoemission spectra as shown in Fig. 3(a). For the secondary electron spectra the kinetic energies relative to the Fermi level are shown. The structures in the secondary electron distribution are related to the unoccupied one-dimensional density of final states (for a given direction) above the vacuum level.

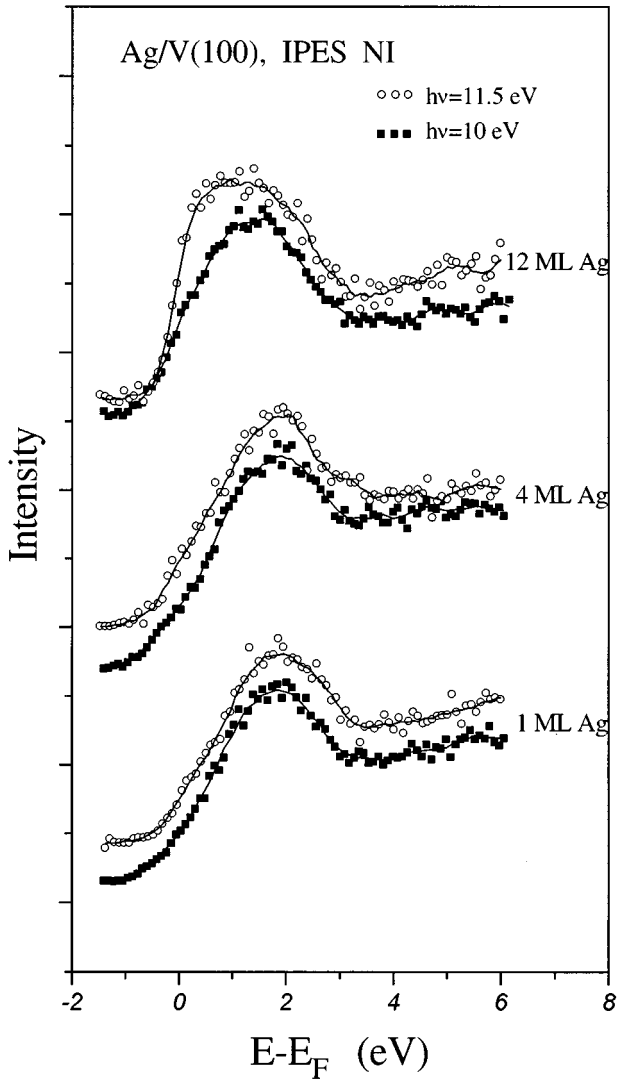

FIG. 6. Normal incidence inverse photoemission (isochromat) spectra of 1, 4 and 12 monolayer films of silver on V(100) recorded at 10.0- and 11.5-eV photon energies.

critical point. From the inflection point associated with the step intensity increase in the top spectrum of Fig. 5(a), we obtain a value for the energy of the X_1 point of 7.60 $\pm$ 0.15 eV above the Fermi level. This is essentially the same as the value (7.5 eV) obtained from a bulk single crystal of Ag(100) (Ref. 10), but is very different from the value reported for silver grown on Fe(100) (5.24 eV).[24] Self-consistent relativistic band-structure calculations[18] for fcc silver give a value of 6.5 eV.

The $X_{4'}$ point can be determined experimentally using inverse photoemission spectra from a thick silver film, assuming that the spectra on their high-energy side reflect the one-dimesional density of states. In Fig. 6 we show that this indeed is the case: Fig. 6 shows normal incidence KRIPES isochromat spectra obtained from different thicknesses of Ag films, recorded at 10.0- and 11.5-eV photon energies. For the thin 1-ML and 4-ML silver films there is no shift in the energies of the Ag-induced states between the two isochromats, consistent with the behavior to be expected for localized surface states or QW states (see below for a further discussion of this point). By contrast, the KRIPES isochromats of the thickest (12-ML) film show a significant photon-energy dependence. The spectrum recorded at 10.0 eV is dominated by a peak at $\approx$ 1.0 eV, while the 11.5-eV spectrum shows a significant intensity increase closer to the Fermi level. The difference between the two KRIPES isochromats can be explained in terms of formation of the bulk Ag Δ_1 band; direct optical transitions between the two branches of this band (indicated with arrows in Fig. 7) then reflect the dispersion of this band. For this coverage the KRIPES data thus imply that both the initial and the final states may be regarded as quasicontinuous bulklike bands. As the 11.5-eV inverse photoemission transition appears to be very close to the ''Fermi level crossing'' condition, the intensity near the Fermi level in the 12-ML film spectrum is attributed mainly to the direct transition, while the rest of the intensity comes from the transitions from evanescent initial states. Under these conditions, the high-energy part of the spectrum reflects the one-dimensional DOS, in which case, the intensity drop-off in the 11.5-eV isochromat seen at $\approx$ 2.5 eV above the Fermi level should correspond to the upper edge of the lower branch of the Δ_1 band at $X_{4'}$. Taking the energy of the inflection point on the edge as that corresponding to $X_{4'}$, we obtain a value of 2.5 $\pm$0.3 eV above E_F. This is somewhat higher than the value of 1.9 eV obtained from similar measurements from bulk fcc Ag(100) single crystals,[31] and the calculated value of 2.2 eV.[18] Of course,

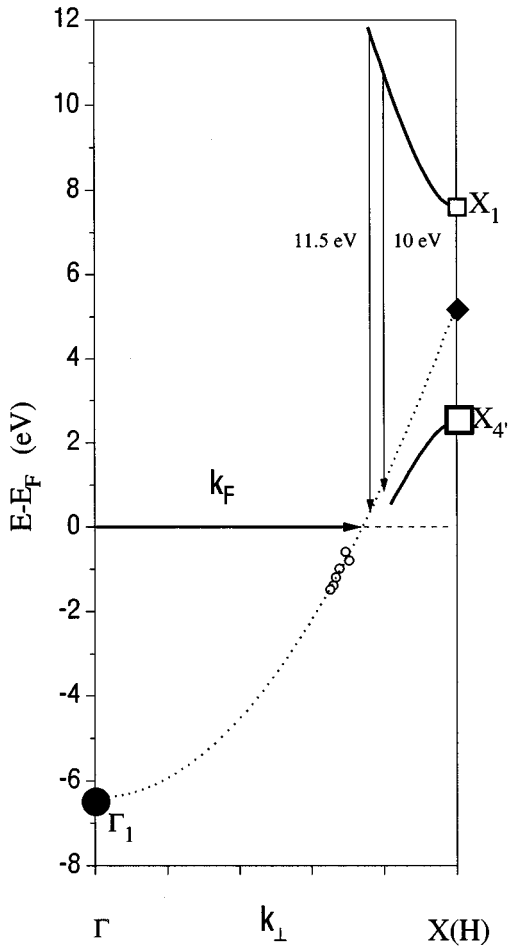

FIG. 7. Schematic bulk-band-structure of the s-p Δ_1 band of tetragonal centered silver produced by pseudomorphic growth on V(100). The experimentally determined points are $X_{4'}$, from the inverse photoemission spectrum of a thick silver film (shown as an open square); and X_1, from the inflection point in the secondary electron distribution of the photoelectron spectra of a thick Ag film (shown as an open square). The points inside the energy region of the Δ_1 gap of the V substrate (open circles) are derived from the photoemission spectra in Fig. 3(a) using a procedure described in the text and Ref. 23. The Γ_1 point (shown as a filled circle) is obtained from the best fit of these points and the point ◆ at the center of the gap to a free-electron model. The corresponding errors are represented by dimension of a particular point in the figure; their values are given in the text.

our experimental values relate not to bulk fcc Ag, but to the pseudomorphic (tetragonally centered) form of Ag associated with growth on V(100).

Assuming that the transport of electrons in these pseudomorphic Ag films is independent of thickness, we can use the measured energies of the experimentally observed QW states in the thin films to determine the Δ_1 band dispersion of this form of Ag in the energy range of their appearance. The procedure for doing this has been described by Lindgren and Wallden.[23] The method exploits the fact that there are QW states with nearly the same energy for different film thickness (e.g., b_1 and c_3). This fact allows us to determine the value of the combined phase shift $(\Phi_B+\Phi_C)$ and the wave vector k of the QW states at this energy inside the film from Eq. (1).[23] If the surface and interface effects are ignored (as they can be for sufficiently thick films), the wave vector k corresponds to the perpendicular wave vector $k_\perp$ of the Bloch state inside a centered tetragonal (CT) Ag bulk sample. This quantity cannot, of course, be determined by photoemission from a bulk sample.

At this point in our discussion it is appropriate to comment on the conditions required for photoemission out of, or inverse photoemission into, surface states and QW states. In the case of a conventional surface state it is usual to regard $k_\perp$ as a meaningless parameter and to take the view that there is no requirement on the conservation of this quantity. In principle this implies that such states should be equally easily seen in ARUPS or KRIPES at the same energy independent of photon energy. In the case of the QW states, on the other hand, k, which is uniquely defined (quantized) in Eq. (1), is equated with $k_\perp$ in the above procedure. If $k_\perp$ for the QW state is quantized, it should be conserved in the optical transitions, with the consequence that the states should only be seen when the photon energy is such as to photoemit into, or have inverse photoemission from, a continuum state of the appropriate $k_\perp$. In reality, this distinction is only quantitative rather than qualitative. In order to evaluate the matrix element for the optical transition to, or from, a continuum state defined by a particular $k_\perp$ (i.e., a single plane wave) one must expand the surface or QW state into plane waves, and because of their high degree of localization perpendicular to the surface, this results in a range of plane waves of differing $k_\perp$. Even for a surface state this range peaks at a particular value of $k_\perp$, especially if the surface-state wave function has an oscillatory tail penetrating the solid, and this leads to enhancement of the matrix element for the optical transition at the appropriate $k_\perp$ value in the matching continuum state.[35,36] In the case of the QW states, the value of k is uniquely defined by the quantization condition, but the finite (but more extended) localization of the state perpendicular to the surface still means that there is a significant probability of optical matching to this state with values of $k_\perp$ spread around the value of k, because again a range of plane waves is needed to describe the localized wave function. Evidently as the layer thickness increases, the localization of the QW state decreases and the demands of $k_\perp$ conservation become increasingly stringent. This means that in ARUPS or KRIPES experiments conducted at single photon energies, the probability of observing the QW state from the thinnest films remains significant at all photon energies, but as the film thickness is increased the visibility of the large number of possible QW states will increasingly favor those states for which the photon energy provides the optimal $k_\perp$ matching. Even for the rather-thin-film QW states, however, the k values deduced from the method of Lindgren and Wallden[23] described above will provide a good estimate of $k_\perp$ for the thick-film state of the same energy.

Using the ARUPS data given here, together with the analysis method of Lindgren and Wallden,[23] we have therefore determined the Δ_1 band dispersion in CT Ag around E_F. Writing Eq. (1) for two different states, observed at the same (or nearly the same) energy, but at different film thickness, we obtain the phase shift $(\Phi_B+\Phi_C)$ and the wave vector k, expressed as a difference in thickness (N_2-N_1) at

which the states are observed. As can be seen in Fig. 4, there are no overlayer states at strictly the same energy, but by interpolating the energy of the overlayer states to noninteger film thicknesses (solid lines in Fig. 4), it is possible to apply this procedure to a continuous-energy range. From the separation of two solid lines in Fig. 4, it is possible to determine $E(k)$ for an arbitrary point in the energy range (below E_F) from -1.6 eV to approximately -0.6 eV. Despite the obvious imprecision in the exact location of the data points in Fig. 4, the values of $k_\perp$ that can be deduced are rather precise. In particular, if we assume that the precision in energy is $\pm$ 0.1 eV, we obtain a value for the layer spacing separation N' between branches b and c of the figure of 3.7 ± 0.2 atomic layers, but the fractional precision in electron momentum δk is given by $(\delta N'/N')[1/(N'-1)]$ or only 2% in this case. The resulting points are shown in Fig. 7. The Fermi wave vector k_F for the overlayer silver estimated from Fig. 7 has a value of $\approx 0.74\ \Gamma H$ (CT) or approximately 1.19 Å^{-1}. This is very close to the de Haas–van Alphen value of 0.819 ΓX (fcc) (or 1.26 Å^{-1}) for fcc silver.[33] The Fermi wave-vector value of 0.74 ΓH (CT) suggests[30] a periodicity of appearance of QWS at the Fermi level of 3.8-ML silver. Since the density of states at the Fermi level is important for transport and magnetic properties of a system, this finding should be taken into account when designing Ag multilayer structures with targeted properties.

We are also able to estimate the position of the bottom of the Δ_1 s-p band, i.e., the Γ_1 point. To do this we have fitted a simple free-electron parabolic dispersion curve through the $E(k)$ points determined experimentally from the occupied quantum wells (see Fig. 7) and a point placed in the middle of the s-p gap at the zone boundary $[(X_{4'}+X_1)/2 = 5.05 \pm 0.23$ eV, marked as a solid diamond in Fig. 7]. The crossing of the best-fit parabola at the zone center ($k_\perp = 0$) corresponds to the Γ_1 point (marked as a solid circle in Fig. 7) and is found at -6.4 ± 0.3 eV (relative to E_F). For comparison, the calculated depth of the s-p band for bulk fcc Ag is -7.21 eV,[32] while the reported value for Ag grown on Fe(100) is much smaller (-5.5 eV).[24] All of the experimentally determined points close to the zone boundary (X) can be fitted with a nearly-free-electron-like dispersion (shown as the thick solid lines in Fig. 7). The lowest Fourier component (V_G) of the periodic potential along the Γ-Δ-$H(X)$ direction, which corresponds to half the band-gap width at the zone boundary ($X_1 - X_{4'}$) is approximately 2.5 eV. The upper branch of the Δ_1 band in Fig. 7 was obtained by drawing a simple nearly-free-electron dispersion through the X_1 point.

B. Cu/V(100)

The large (16%) lattice mismatch between the (100) face of fcc copper and the (100) face of bcc vanadium has a crucial influence on the growth of Cu on V(100). Only Cu films with a thickness of no more than two layers are found to show some degree of pseudomorphic ordering. With increasing thickness, the films become gradually more and more disordered, and we can expect to see the influence of this disorder on the QW states in photoemission and KRIPES data. Figure 8 shows the normal emission photoemission spectra, and the normal incidence KRIPES data recorded

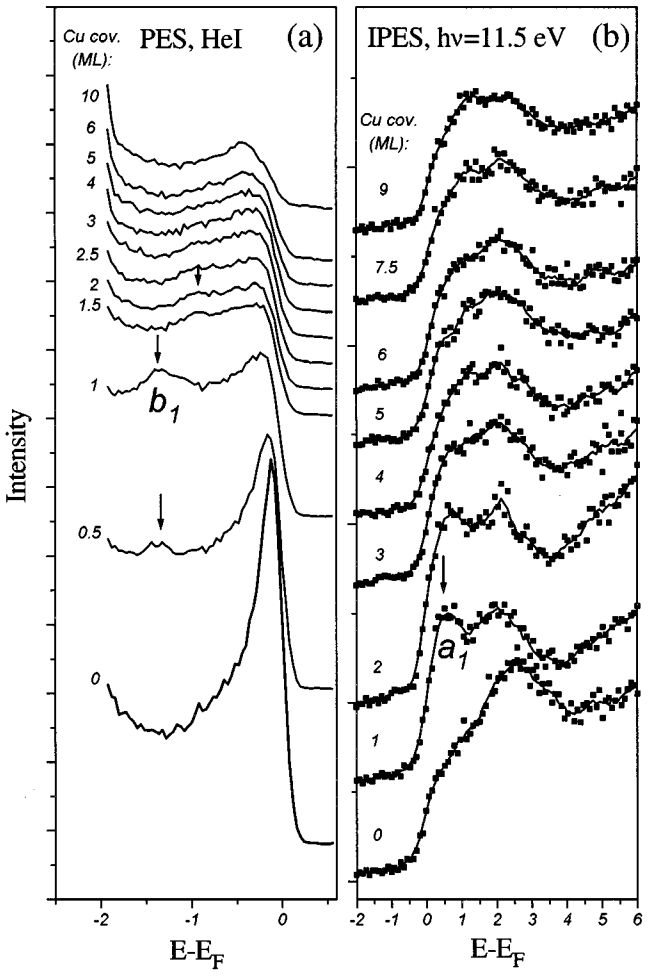

FIG. 8. Normal emission photoelectron (a) and normal incidence KRIPES isochromat spectra (b) from Cu films of various thicknesses (given in ML) on V(100).

from copper films of various thicknesses grown on V(100). Only two Cu-derived states are clearly resolved in the photoemission spectra: one at -1.4 eV (from a film with a thickness of 1 ML), and the other at -0.9 eV (at 2-ML thickness). On the basis of model calculations similar to those of Ref. 24 for the energy of QW states, we found that the observed states can be assigned as b_1 and b_2 ($\nu = 1$). In the KRIPES data only one relatively sharp overlayer state can be recognized at approximately 0.6 eV above E_F from the 1-ML film. This feature appears at a slightly higher energy for the 2-ML film and gradually disappears for thicker films, and can be assigned as the a_1 ($\nu = 0$) overlayer state. The b_1 state is actually seen at submonolayer coverages but shifts slightly to higher energy with increasing coverage up to 1 ML; this may be attributed to the effect of the significant (0.4-eV) work function increase, which has been found to occur during the growth of the first monolayer.[16] As a consequence, the same barrier phase shift Φ_B is reached at a slightly higher energy [see Eq. (2)], while all other parameters in Eq. (1) remain unchanged, i.e, the quantization condition (1) shifts the same monolayer state to higher energy. Although the work-function change affects higher states much more strongly

(these higher states are almost fixed in energy relative to the vacuum level due to the divergence of Φ_B as it approaches the vacuum level), a measurable shift (0.1–0.2 eV) can be observed even for the state at 1.4 eV below the Fermi level. Obviously, for the systems where large work-function changes are observed, these effects cannot be ignored.

Although these data provide evidence for QW states in the thinnest, reasonably ordered Cu films, the poor order of the thicker films precludes any possibility of performing an analysis of the dispersion of a possible bulklike Cu *s-p* band as we have done for the silver layers. Similarly, there are insufficient data to follow the emergence of QW states with increasing thickness akin to those for Ag films shown in Fig. 4. Furthermore, the secondary electron distribution from thick Cu films showed no distinct step structure that could be attributed to the band edge, which we could expect for a well-ordered film.

C. Low coverage limit of Ag and Cu films

For the thinnest overlayer films, the electronic structure can be strongly influenced (in comparison with the bulk) by the lowered symmetry, reduced atomic coordination, and hybridization with the electronic states of the substrate. These effects can be expected to be of least influence for more localized states of the overlayer. In our case it is clear that photoemission data [Fig. 5(b)] from the relatively localized Ag 4*d* states converge at quite low thicknesses (3–4 ML) to that of the bulklike band. For the more delocalized *s-p* states, on the other hand, it is only for thicknesses of approximately 10 ML or more that this region of the spectrum becomes characteristic of the bulk (see Fig. 3 for silver; Fig. 8 for copper).

The simple quantum-well model, which we have used extensively in the discussion of our results, is based on the quantization of bulklike states, so we might expect it to break down when going to small thicknesses. This effect has been observed in some systems as a departure of the overlayer states energies from those predicted for QW states when approaching the monolayer limit.[5,10,11] For other systems, however, the quantum-well states converge to substrate *s-p* surface resonances even in the zero coverage limit.[12,24] In our study of Ag and Cu films on the V(100) surface, the energies of the QW states are found to be in good agreement with those predicted by the simple quantum-well picture down to the monolayer limit (at least for the $\nu=1$ state). Furthermore, the simple phase-accumulation model,[6–8] originally devised for the theoretical description of *s-p* surface states, gives the correct energies for the overlayer states if one includes the proper input parameters for the energetic positions of the substrate Δ_1 band gap and a realistic description of the dispersion with $k_\perp$ of the overlayer *s-p* band in the bulklike limit.

Despite this success of the simple theoretical description of the QW states, measurements of the dispersion of these states with $k_\parallel$ do appear to show a significant deviation from the expected[34] free-electron-like behavior. The experimentally determined $k_\parallel$ dispersion of some overlayer states, and also of selected vanadium bulk bands, in the [011] direction is presented in Fig. 9 while Fig. 10 displays ARPES spectra showing the dispersion of the b_2 state of the 2-ML Ag and

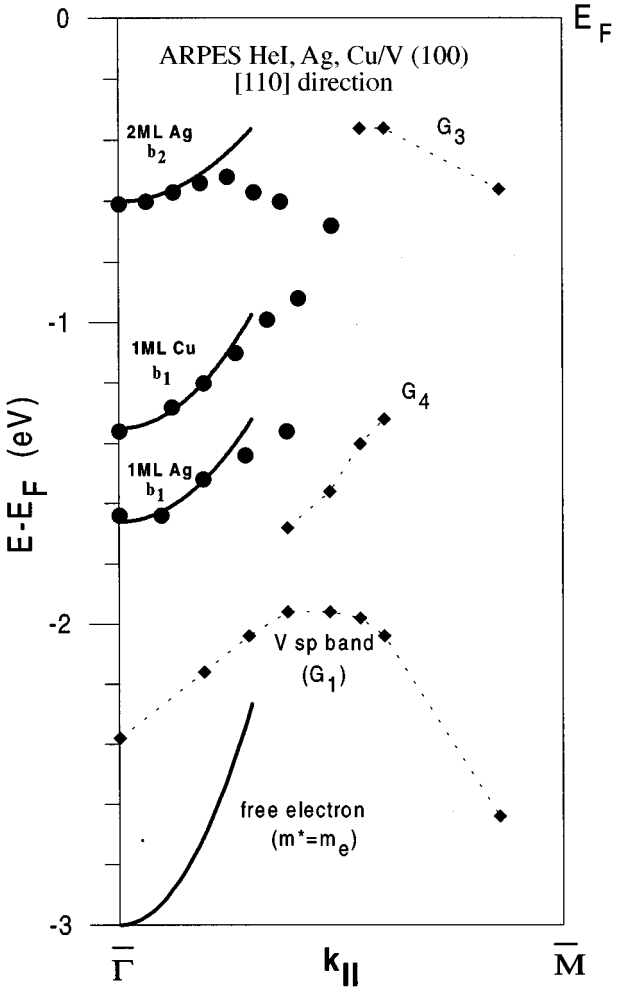

FIG. 9. Experimentally determined dispersion of some overlayer QW states ($\nu=1$ states for 1 ML and 2 ML of Ag and for 1 ML of Cu) as a function of $k_\parallel$, measured along the $\bar{\Gamma}$-$\bar{M}$ symmetry line of the surface Brillouin zone. The solid lines show the best-fit parabolic dispersion curves (with various values of m^*) near the center of the surface Brillouin zone. A free-electron-like dispersion curve ($m^* = m_e$) is shown for comparison. For a better insight into possible hybridization with the substrate bands, the experimentally determined points in dispersion of the vanadium bulk bands, along the same symmetry line, are shown as diamonds.

b_1 state of 1-ML Cu film. A departure from free-electron-like dispersion ($m^* = m_e$) is obvious. Even near the zone center, the dispersion is considerably weaker than the free-electron-like behavior. The electron effective masses obtained from the fits shown in Fig. 9 to the $\nu=1$ states in the proximity of the $\bar{\Gamma}$ point are $2.2m_e$ and $3.1m_e$ for 1 ML and 2 ML of silver, respectively, and $1.9m_e$ for 1 ML of copper. Such a large effective mass typically indicates strong hybridization with more localized states (with larger effective mass) in the substrate. One possible candidate for such an effect is a mixing with the *s-d* substrate band outside the gap. This band has mainly *d* character near the gap, and consequently, a large effective mass. The extension of a QW wave function into the classically forbidden region outside

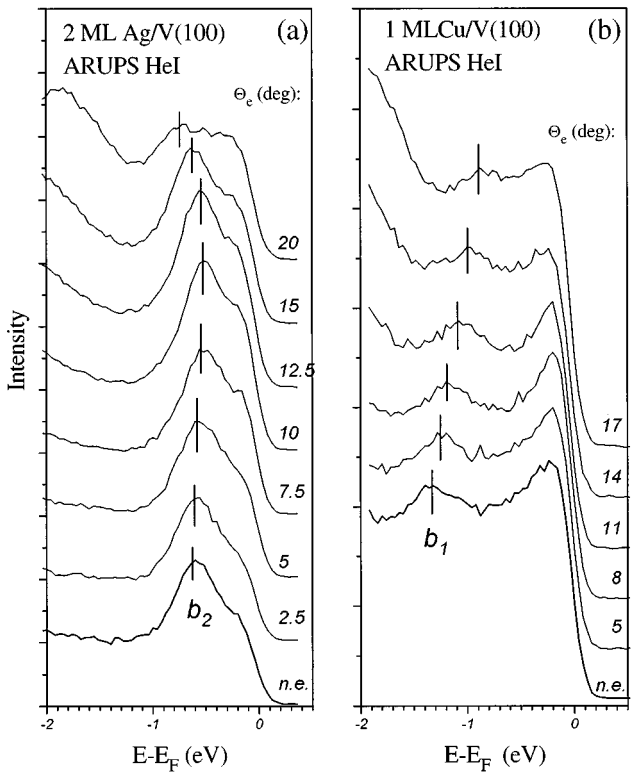

FIG. 10. ARUPS spectra of (a) 2-ML Ag and (b) 1-ML Cu film showing the dispersion of b_2 and b_1 QW states, respectively, along the $\bar{\Gamma}$-$\bar{M}$ symmetry line of the surface Brillouin zone in the vicinity of the center of the surface Brillouin zone.

the well is largest for the states closest to the gap edge. It is thus notable that the 1-ML Ag state is the nearest in energy to the gap edge; in addition, the influence of the interface should be most pronounced in the monolayer case. We might therefore expect the strongest departure from the anticipated free-electron-like behavior for the QW state in the 1-ML film. However, the data of Fig. 9 and the calculated effective mass indicate that an even greater deviation occurs for the 2-ML film. This implies that hybridization with the more localized vanadium d bands inside the Δ_1 gap may play a significant role. The dispersion of the 2-ML Ag state (Fig. 9) strongly supports this possibility; it changes the sign on moving away from $\bar{\Gamma}$ towards $\bar{M}$, an effect that could be a consequence of strengthening hybridization with the G_3 vanadium $3d$ derived band (which has negative dispersion in this region). The 1-ML Cu state possesses the lowest effective mass, implying the lowest degree of hybridization. We should add that, as all of the QW states mapped in Fig. 9 fall in the lower half of the substrate band gap, it is not possible to account for the high apparent effective masses in terms of a kind of repulsion of the bulk band edge due to the shifting Φ_C in the dispersing gap, as has been seen in image potential states on certain metal surfaces;[7] indeed, in the lower half of the gap, this effect can only lead to an enhancement of the $k_\parallel$ dispersion and thus a reduction of the apparent effective mass.

IV. CONCLUSIONS

We have shown that for silver and copper films on V(100), discrete overlayer states are formed within the Δ_1 gap of the vanadium substrate. In the case of the Ag/V(100) system, we have observed overlayer states for all examined thicknesses (up to 15 ML). In the case of copper, pseudomorphic growth only occurs to about 2 ML and only three overlayer states have been resolved. We have used the quantum-well model to describe these states. This has enabled us to determine important critical points in the dispersion of the Δ_1 band in the $\bar{\Gamma}$-$\bar{\Delta}$-$\bar{X}$ direction of pseudomorphically grown (tetragonal-centered) silver; the energies of the Γ_1, X_1, and $X_{4'}$ points, as well as the Fermi wave vector k_F, have been determined. Since such a tetragonal centered silver could be an ideal substrate for the transition-metal films (especially for vanadium), establishing its electronic structure is of crucial interest. In the low-coverage limit (1–2 ML) for both Ag and Cu films, we have found a significant enhancement of the electron effective mass ($m^* > 2m_e$) of discrete s-p states for dispersion in $k_\parallel$. This is taken to indicate strong hybridization of these states with the d derived states of the vanadium substrate. We have suggested that the states inside the Δ_1 vanadium gap may be dominant in this hybridization process.

ACKNOWLEDGMENTS

The authors are pleased to acknowledge the financial support of the Ministry of Science and Technology of the Republic of Croatia (Project No. 1-03-056), the Engineering and Physical Science Research Council, in the form of research grant, and the support of the British Council and Croatian Ministry of Science and Technology for the associated Warwick-Zagreb collaboration, which also supported the stay of T. Valla in Warwick. The authors thank Dr. B. Gumhalter for useful discussions.

[1] *Polarized Electrons in Surface Physics*, edited by R. Feder (World Scientific Publishing, Singapore, 1985).

[2] *Magnetic Surfaces, Thin Films, and Multilayers*, edited by S. S. P. Parkin, H. Hopster, J-P. Renard, T. Shinjo, and W. Zinn, MRS Symposia Proceedings No. 231 (Materials Research Society, Pittsburgh, 1991).

[3] J. E. Ortega and F. J. Himpsel, Phys. Rev. Lett. **69**, 844 (1992).

[4] O. Rader, C. Carbone, W. Clemens, E. Vescovo, S. Blugel, W. Eberhardt, and W. Gudat, Phys. Rev. B **45**, 13 823 (1992); T. Kachel, W. Gudat, C. Carbone, E. Vescovo, U. Alkemper, S. Blugel, and W. Eberhardt, *ibid.* **46**, 12 888 (1992).

[5] C. Carbone, E. Vescovo, O. Rader, W. Gudat, and W. Eberhardt, Phys. Rev. Lett. **71**, 2805 (1993).

[6] P. M. Echenique and J. B. Pendry, J. Phys. C **11**, 2065 (1978); N. V. Smith, Phys. Rev. B **32**, 3549 (1985); Rep. Prog. Phys. **51**, 1227 (1988).

[7] N. V. Smith and D. P. Woodruff, Prog. Surf. Sci. **21**, 295 (1986).
[8] P. M. Echenique and J. B. Pendry, Prog. Surf. Sci. **32**, 111 (1990).
[9] E. G. McRae, Surf. Sci. **25**, 491 (1971); J. B. Pendry and S. B. Gurman, *ibid*. **49**, 87 (1975).
[10] J. E. Ortega, F. J. Himpsel, G. J. Mankey, and R. F. Willis, Phys. Rev. B **47**, 1540 (1993).
[11] F. J. Himpsel, Phys. Rev. B **44**, 5966 (1991).
[12] N. Brookes, Y. Chang, and P. D. Johnson, Phys. Rev. Lett. **67**, 354 (1991).
[13] E. Vescovo, O. Rader, J. Redinger, S. Blugel, and C. Carbone, Phys. Rev. B **51**, 12 418 (1995).
[14] T. Valla and M. Milun, Surf. Sci. **315**, 81 (1994).
[15] T. Valla, P. Pervan, and M. Milun, Vacuum **46**, 1223 (1995).
[16] T. Valla, P. Pervan, and M. Milun (unpublished).
[17] D. A. Papaconstantopulos, J. R. Anderson, and J. W. McCaffrey, Phys. Rev. B **5**, 1214 (1972).
[18] H. Eckardt, L. Fritsche, and J. Noffke, J. Phys. F **14**, 97 (1984).
[19] P. Pervan, T. Valla, and M. Milun, Solid State Commun. **89**, 917 (1994).
[20] M. D. Crapper, A. L. D. Kilcoyne, and D. P. Woodruff, Phys. Scr. **41**, 546 (1990).
[21] T. Valla, P. Pervan, and M. Milun, Surf. Sci. **307/309**, 843 (1994).
[22] P. Pervan, T. Valla, M. Milun, A. B. Hayden, and D. P. Woodruff, J. Phys. C **8**, 3705 (1996).
[23] S. A. Lindgren and L. Wallden, Phys. Rev. Lett. **61**, 2894 (1988).
[24] N. V. Smith, N. B. Brookes, Y. Chang, and P. D. Johnson, Phys. Rev. B **49**, 332 (1994).
[25] The quantum-well-state energies have been calculated using a method from Ref 24.
[26] J. A. Knapp, F. J. Himpsel, and D. E. Eastman, Phys. Rev. B **19**, 4952 (1979).
[27] P. O. Nilsson and I. Lindau, in *Band Structure Spectroscopy of Metals and Alloys*, edited by D. J. Fabian and L. M. Watson (Academic, New York, 1973); N. E. Christensen and B. Feuerbacher, Phys. Rev. B **10**, 2349 (1974); B. Feuerbacher and N. E. Christensen, *ibid.* **10**, 2373 (1974).
[28] G. J. Mankey, R. F. Willis, and F. J. Himpsel, Phys. Rev. B **47**, 190 (1993).
[29] G. J. Mankey, R. F. Willis, and F. J. Himpsel, Phys. Rev. B **48**, 10 284 (1993).
[30] If we denote the periodicity at the Fermi level (in layers) as p, then $p=1/1-k_F$, where k_F is expressed as a fraction of the distance to the Brillouin-zone edge.
[31] F. J. Himpsel and J. E. Ortega, Phys. Rev. B **46**, 9719 (1992).
[32] P. D. Loly and J. B. Pendry, J. Phys. C **16**, 423 (1983).
[33] P. T. Coleridge and I. M. Templeton, Phys. Rev. B **25**, 7818 (1982).
[34] H. Erschbaumer, A. J. Freeman, C. L. Fu, and R. Podloucky, Surf. Sci. **243**, 317 (1991).
[35] S. D. Kevan, N. G. Stoffel, and N. V. Smith, Phys. Rev. B **31**, 3348 (1985).
[36] S. D. Kevan, N. G. Stoffel, and N. V. Smith, Phys. Rev. B **31**, 1788 (1985).